International Journal of Materials Science

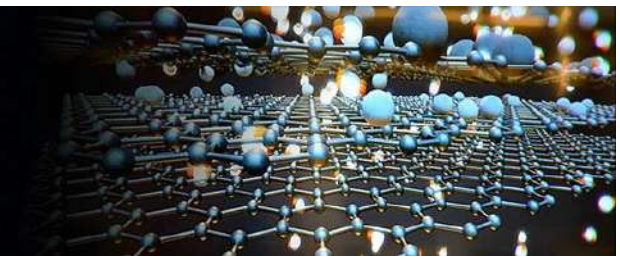

E-ISSN: 2707-823X
P-ISSN: 2707-8221
IJMS 2023; 4(1): 01-11
Received: 04-11-2022
Accepted: 06-12-2022

HHM Darweesh
Refractories, Department of Refractories, Ceramics and Building Materials, National Research Centre, Cairo, Egypt

Corresponding Author:
HHM Darweesh
Refractories, Department of Refractories, Ceramics and Building Materials, National Research Centre, Cairo, Egypt

Effect of banana leaf ash as a sustainable material on the hydration of Portland cement pastes

HHM Darweesh

Abstract
The non-traditional materials as agrowastes like banana leaf ash (BLA) are leading to reduce carbon footprint, gas emissions and agrowaste generation. Hence, the current research article investigates the use of BLA as a partial replacement for ordinary Portland cement (OPC) in eco-friendly cement. On this basis, cement pastes were produced with a partial substitution of BLA by 0, 3, 6, 9, 12 and 15% at the expense of the OPC. The physical properties in terms of consistency, setting, bulk density and water absorption and total porosity as well as the mechanical properties in terms of compressive strength were studied. Results illustrated that the water of consistency and setting times (Initial and final) increased with the increase of BLA content. The bound water content and bulk density improved and enhanced only up to 12%, and then decreased with any further increase of BLA content. On contrast, total porosity decreased as the BLA content increased to 12%, and then increased with the increase of BLA. The free lime test indicated that the BLA could be reacted with evolved Ca $(OH)_2$ fron the normal hydration of the silicate phases of the cement producing additional CSH, due to the pozzolanic potential of the used agrowaste material. This was reflected positively on the compressive strength. Therefore, the blended cement pastes containing 12% BLA had the best significant improvements in its performance and properties. Hence, it was selected as the optimum batch. The FT-IR spectra and SEM images proved that the free lime content gradually decreased with both the incorporation of BLA and time of hydration followed by the formation of additional CSH. This was reflected positively on the mechanical properties.

Keywords: Cement, BLA, consistency, setting times, density, free lime, pozzolanic activity, strength

Introduction
It is well known that about 10-15% or little more of concrete volume is cement. Some reports pointed that in 2019 about 4.1 gigatons of Portland cement were consumed [1, 2]. Most of this consumption goes to produce concrete. On the other hand, approximately 7-10% of CO_2 emissions in the world come from PC production [3]. This is mainly due to the process of decarbonation of limestone rock that is responsible for about 60% of CO_2 emissions on the planet [4]. At all, cement industry is responsible for the emission of > 1.5 GigaTons of CO_2 into the atmosphere [5]. This sertainly led to the generation of a series of problems associated with the depletion of natural resources and increase in global greenhouse gas emissions [6]. In this perspective, it is necessary to search new alternatives that help to use new materials with a smaller carbon footprint to replace PC. Therefore, this could be contributet to a cleaner production.
In recent years, many scientific researchs on waste incorporation in cement and/or concrete using solid wastes as filler or pozzolanic materials have been conducted to promote the use of materials that can reduce the environmental impact of CO_2 emissions from cement production [1], which can be used in the form of ashes and/or fibers to replace PC. A variety of organic materials have been investigated, as rice husk ash [7–13], sugarcane bagasse ash [14-18], cotton stalk ash [18, 19], palm oil ash [9, 20–27], wood ash [28–30], elephant grass ash [31], crushed walnut shell [32], olive waste ash [33], cattle manure ash [34] and banana leaf ash [35, 36]. Although there are many researches with agroindustrial biomass residue ashes being used in eco-friendly concretes, there is a challenge in making these alternative materials feasible in the context of the construction industry. The lack of advanced researches and exploitation of agrowaste ashes in different types of concretes [25], the need for appropriate and field applications are necessary to enable the worldwide diffusion of green concrete [37, 38].
The banana leaf ash (BLA) stands out for being a widely available and little investigated material.

The production of banana involves the generation of a high volume of waste, which is associated with losses inherent to the production. The pozzolanic activity of mechanically activated BLA was studied by analyzing the compressive strength of lime and OPC based mixtures [35]. The BLA meets the normative requirements where the ideal grinding time is 30 min. Continuing the studies on the subject, Also, the rheological performance of mortars with 0–10% of BLA replacing OPC and the mechanical and durability performances for concrete samples with 10–20% of BLA, also replacing PC [36]. Results showed that the mechanical strengths at 28 days of concrete with 10% and 20% of BLA were 25% and 40% higher than the reference concrete (0% of BLA), respectively. It is evident from some studies that there is a need to study and evaluate the effects of different levels of BLA at the expense of OPC, and to highlight its action and ecological importance. So, the main target of this study is to evaluate the effects of partial replacement of PC by 0, 5, 10, 15 and 20% of BLA on the physical, chemical, mechanical and microstructural properties of concrete.

Experimental

Raw materials

The used raw materials in this study are ordinary Portland cement (OPC) and banana leaves (BL). The OPC sample (OPC Type I- CEM I 42.5 R) was delivered from Sakkara cement factory, Giza, Egypt, and its commercial name is known as "Asmant El-Momtaz". After collection of BL, it was calcined at a temperature of 900 ºC using a muffle furnace for two hours soaking time. The calcination helps to eliminate the organic compounds from the leaves to initiate its use as a pozzolanic material. The resulting material was let to grind in a ball mill for only 30 minutes till pass from a 75 µm sieve (Fig. 1). The surface area or fineness of PC and BLA as determined by the Blaine air permeability apparatus (BPA) were 3500 and 5950 cm^2/g, respectively. The specific gravities of OPC and BLA as measured with a Le Chatelier flask were 3.15 and 2.65 g/cm^3, respectively. The chemical analysis of OPC and BLA using X-ray Fluorescence technique (XRF) is shown in Table 1. To achieve the pre-established reference consistency, it was necessary to add 1% polycarboxylic ether as a high reducing water superplasticizer admixture to the mixing water. Table 2 shows the Mineralogical composition of OPC sample, while Table 3 indicates the physical properties of the raw materials.

Table 1: Chemical oxide composition of the raw materials, wt.%

Oxides Material	SiO_2	Al_2O_3	Fe_2O_3	CaO	MgO	Na_2O	K_2O	SO_3	LOI
OPC	20.12	5.25	1.29	63.13	1.53	0.55	0.3	2.54	2.64
BLA	30.56	8.31	3.68	51.73	3.67	0.02	1.09	0.07	0.71

Table 2: Mineralogical composition of OPC sample, wt.%.

Phase Material	C_3S	β-C_2S	C_3A	C_4AF
OPC	46.81	28.43	5.90	12.56

Table 3: Physical properties of the raw materials, wt%

Properties Materials	Specific gravity	Density, g/cm^3	Blaine surface area, cm^2/g
OPC	3.15	1445	3500
BLA	2.66	1248	5950

Fig 1: Banana tree: (A) Banana leaves, (B) Banana leaf Ash (BLA).

Preparation and methods

There are 6 cement batches from OPC and BLA as 100:0, 97:3, 94:6, 91:9, 88:12 and 85:15 having the symbols: B0, B1, B2, B3, B4 and B5, respectively. The blending process of the various cement blends was done in a porcelain ball mill using three balls for two hours to assure the complete homogeneity of all cement blends. During casting, 1% polycarboxylic ether as a high reducing water superplasticizer admixture was added to the mixing water which in tuern added to the prepared cement mixes so as to avoid the agglomeration of the nanoparticles of the used BLA or OPC. It was applied due to its higher activivity than other conventional ones, which contains several free carboxylic groups that helps greatly to improve cement dispersion.

The standard water of consistency (WC) as well as setting time (initial and final) of the various cement pastes were directly determined using Vicat Apparatus [39-42]. The cement pastes were then cast using the predetermined water of consistency, moulded into one inch cubic stainless steel moulds (2.5 x 2.5 x 2.5 cm^3) using about 500 g cement mix, vibrated manually for three minutes and then on a mechanical vibrator for another three minutes. The surface of the moulds was smoothed using a suitable spatula. Thereafter, the moulds were kept in a humidity chamber for 24 hours under 95±1 RH and room temperature, demoulded in the next day and soon immersed in water till the time of testing at 1, 3, 7, 28 and 90 days. The bulk density (BD) and

total porosity (δ) of the hardened cement pastes [40-42]. The compressive strength (CS) of the various hardened cement pastes [43] was measured.

Thereafter, about 10 grams of the broken specimens were first well ground, dried at 105 °C for an hour, and then were placed in a solution mixture of 1:1 methanol: acetone to stop the hydration [44, 45]. About 10 grams of the broken specimens from the determination of compressive strength were first well ground, dried at 105 °C for 30 min., and then were placed in a solution mixture of 1:1 methanol: Acetone to stop the hydration [44, 45]. The chemically-bound water content was measured, where bout one gram of the sample was first dried at 105 °C for 24h, and then the chemically-bound water content (BWn) at each hydration age was determined on the basis of ignition loss at 1000°C for 30 min. soaking [39-42, 46].

The pozzolanic activity was detected by measuring the free lime content (FLn) of the hydrated samples pre-dried at 105°C for 24h. About 0.5 g of the sample + 40 ml ethylene glycol → heating to about 20 minutes without boiling. About 1–2 drops of pH indicator were added to the filtrate and then titrated against freshly prepared 0.1N HCl until the pink colour disappeared. The 0.1N HCl was prepared using the following equation: Where, Wn, W1 and W2 are combined water content, weight of sample before and after ignition, respectively. The free lime content of the hydrated samples pre-dried at 105°C for 24h was also determined. About 0.5g sample +40 ml ethylene glycol → heating to about 20 minutes without boiling. About 1–2 drops of pH indicator were added to the filtrate and then titrated against freshly prepared 0.1N HCl until the pink colour disappeared. The heating and titration were repeated several times until the pink colour did not appear on heating [38, 44, 45].

The DTA-TGA analysis was carried out using NETZSCH Geratobau Selb, Bestell-Nr. 348472c at a heating rate 10 °C/min up to 1000 °C. The electrical conductivity test [47, 48] consisted of measuring the electrical conductivity at pre-set times in a solution with 0.45 g of calcium hydroxide, 250 ml of deionized water and 5.25 g of the BLA. The relative difference in conductivity for a given time is determined as a function of the initial conductivity. Based on the electrical conductivity values proposed by Lux´an [47] the materials are classified according to their pozzolanicity. The obtained results are confirmed with fourier transform infared spectra (FT-IR) and scanning electron microscopic (SEM) analysis. The FT-IR was performed by Pye-Unicum SP-1100 in the range of 4000-400 cm^{-1} and a resolution of 500 cm^{-1}. The FT-IR analysis was done in the National Research Centre, Dokki, Cairo, Egypt. The SEM microscopy was conducted for some selected samples by using JEOL–JXA–840 electron analyzer at accelerating voltage of 30 KV. The fractured surfaces were fixed on Cu-kα stubs by carbon paste and then coated with a thin layer of gold.

Results and Discussions

Characterization of BLA

The BLA is essentially composed of silicon oxide (SiO_2) and calcium oxide (CaO). The SiO_2 of BLA is very active, since it can react with the calcium hydroxide Ca $(OH)_2$ or free lime evolved during the hydration of cement phases to produce additional calcium silicate hydrate (C–S–H) [49–51]. Hense, this was reflected on the mechanical properties of cementitious materials. A small amount of alumina (Al_2O_3) and iron oxide (Fe_2O_3) have been identified. Sum of pozzolanic oxides (SiO_2 + Al_2O_3 + Fe_2O_3) of the BLA is compatible with the chemical requirements established with ASTM C618-12 [52]. The sum of these oxides should be at least 50% to be classified as class E ashes [42, 43]. The alkali oxldes (K_2O and Na_2O) as well as Cl^- ions are probably associated and may be contributed to the occurrence of the alkali-aggregate reaction [53] and development of chloride attack. However, these compounds may be important in alkali activated mixtures [54]. The X-ray diffraction patterns of BLA are shown in Figure 2. The main crystalline phases of the BLA are quartz (SiO_2) and calcite ($CaCO_3$). Some other phases with lower intensity are present, such as iron and chlorite. The presence of the KCl phase may be due to the use of fertilizers in the soil. The presence of crystalline phases in BLA may be due to the slow cooling till reach to the room temperature [36]. However, an amorphous halo was identified which may favor the development of pozzolanic reactions, where the BLA showed a large amorphous degree [35]. These notes are consistent with inherent characteristics of agricultural ashes [36, 51].

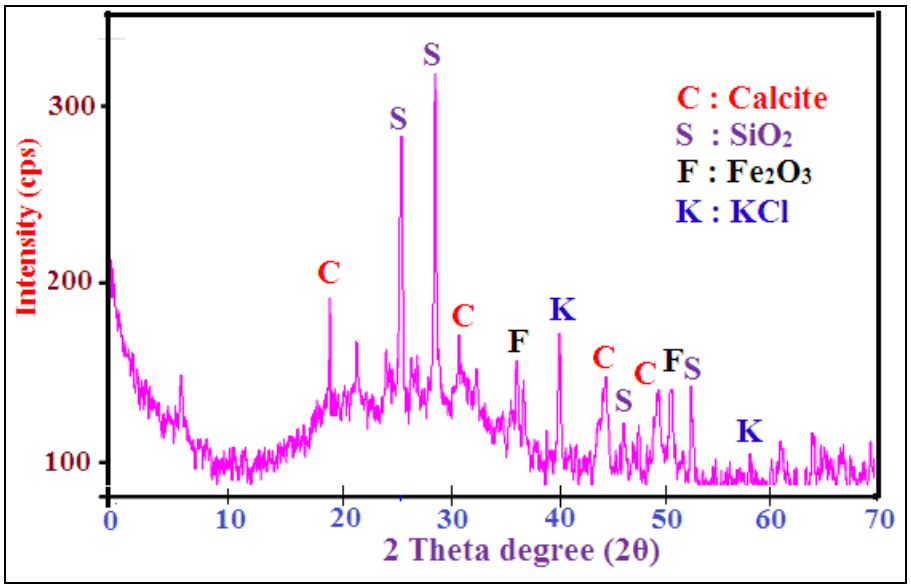

Fig 2: X-ray diffraction patterns of the BLA.

Figure 3 illustrates thermogravimetric analysis (DTA and DTG) of the BLA. At 900 ºC, the BLA material presents a considerable weight loss, which favors its pozzolanic potential. At high temperatures, the transition of amorphous silica into cristobalite had taken place [55, 56], which prevent the occurance of the pozzolanic potential of the BLA. Between 150 and 420 ºC, the hemicellulose and/or cellulose had been degraded. At 420 to 900 ºC, the lignin of BLA would beed degraded completely till the total formation of ash [57]. Concerning the differential thermal analysis (DTA) of the BLA, few endothermic and exothermic thermal peaks were identified. At the temperatures range of 0-450 ºC, some endothermic peaks appearred due to weight loss of water and volatiles. At 590-630 ºC, an exothermic peak was identified. This means that a possible degradation of the material [58].

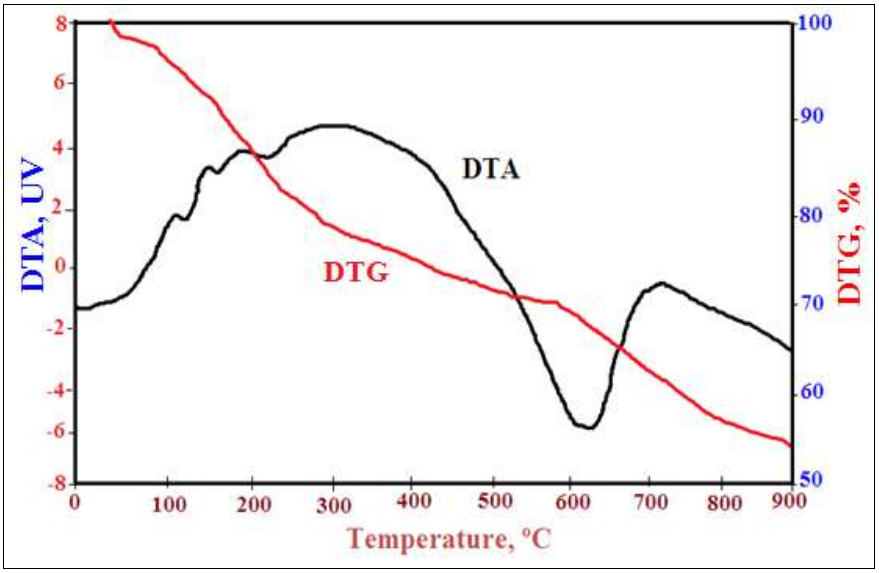

Fig 3: DTA and DTG of the BLA material.

The electrical conductivity test for BLA is shown in Fig. 4. The electrical conductivity of the solution of BLA decreased with time. This is mainly attributed to the fixation of calcium hydroxide Ca $(OH)_2$. This in turn led to the formation of insoluble products [59]. This also indicates and initiates the pozzolanic potential of the BLA. Moreover, the difference in the electrical conductivity between the final and initial times was 1.9 mS/cm, which is considered as a good pozzolanic material which is >1.2 mS/cm as concluded by Pay´a *et al*. [48].

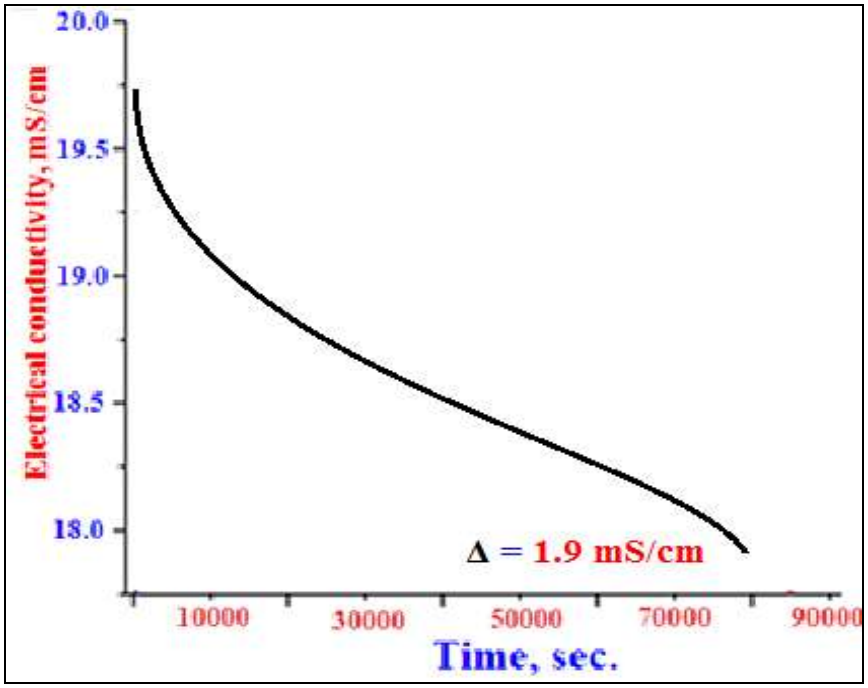

Fig 4: Electrical conductivity curve for BLA.

Physical properties

Water of consistency and setting time

The water of consistency and setting times (initial and final) of the various cement pastes with and without BLA (B0-B5) are represented in Fig. 5. As it is clear the water of consistency increased as the BLA content increased. This is essentially due to the fact that the B LA likes water so much to form standard cement pastes [39-42]. The same trend was

displayed by the setting time. Therefore, the BLA is very voracious for water. The measured water of consistency was used in all tests.

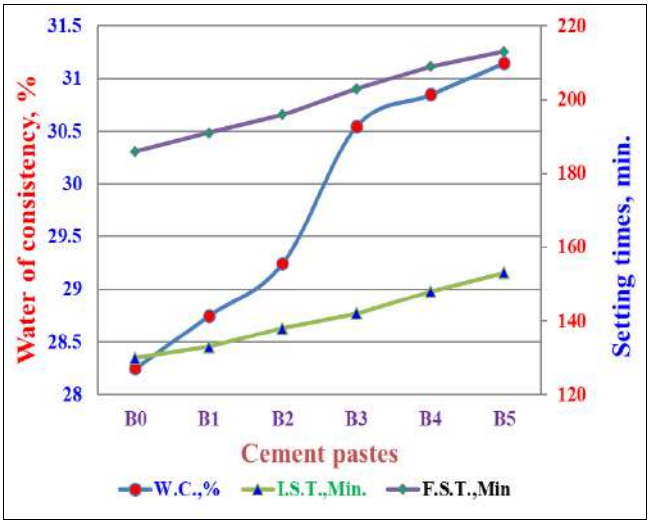

Fig 5: Water of consistency and setting times (initial and final) of the various cement pastes with and without BLA.

Water absorption

The results of water absorption (WA) of the hardened cement pastes at 1, 3, 7, 28 and 90 days are shown in Fig. 6. Generally, the WA of the reference sample (B0) was 28.25%. This value was decreased with the incorporation of BLA only up to 12% (B4), and then slightly increased with the further increase of BLA content (B5). The decrease of WA is mainly contributed to the higher compaction effect by higher surface area or fineness of the BLA particles which reflected positively where it reduced the pore volume of the hardened cement pastes [44, 45]. The increase of WA is essentially attributed to the large deficiency of the main binding material [60, 61]. Consequently, the greater amount of this waste must be avoided.

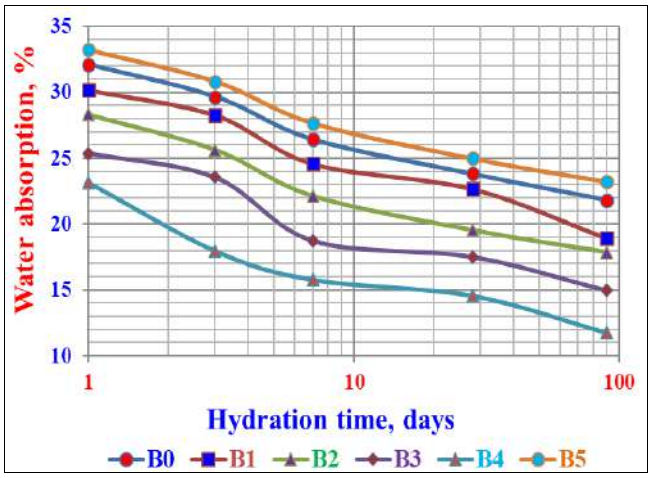

Fig 6: Water absorption of the various cement pastes with and without BLA hydrated up to 90 days.

Total porosity

Figure 7 showed the values of total porosity of the hardened cement pastes of the different cement pastes with and without BLA (B0-B5) cured up to 90 days. The total porosity of the reference (B0) at any hydration time was decreased with the increase of BLA content, but only up to 12%, and then reincreased with any further addition of BLA (B5). The decrease of total porosity is principally due to the hydration of the main phases of the cement [8-11]. Moreover, the pozzolanic reactivity of BLA with the resulting Ca $(OH)_2$ coming from the normal hydration process of the silicate phases of the cement producing additional CSH that precipitated into the pore structure. This reduced the total porosity [39, 44, 45]. The reincreased values of the total porosity with higher content of BLA than 12% (B5) is mainly attributed to the larger deficiency of the main binding material which is responsible for the hydration process [39, 40, 62]. So, the higher content of BLA than 12% must be avoided.

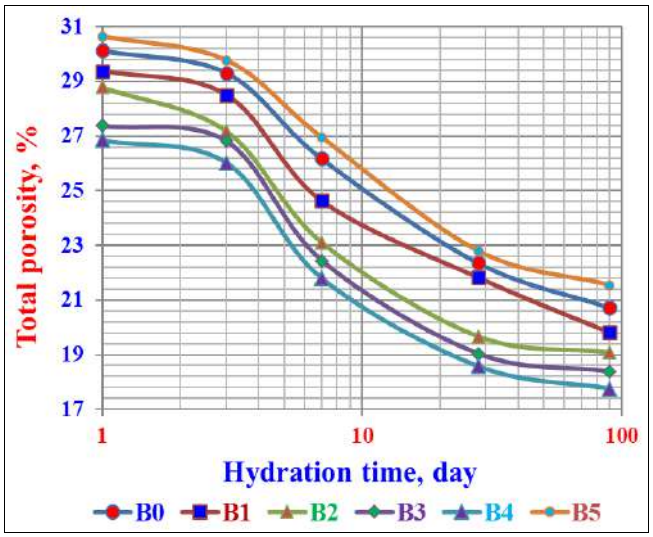

Fig 7: Total porosity of the various cement pastes with and without BLA hydrated up to 90 days.

Bulk density

The results of bulk density of the various hardened cement pastes with and without BLA (B0-B5) hydrated up to 90 days are presented in Fig. 8. Generally, the bulk density slightly increased with the incorporation of BLA till 12% (B4), and then decreased by the further increase of BLA (B5). The increase of bulk density is mainly due to the deposition of the formed CSH from the hydration of the main phases of the cement and also the additional CSH that resulted from the pozzolanic reactions of BLA particles with the free lime, Ca $(OH)_2$ coming from the hydration of the calcium silicate phases of the cement [44, 45, 62]. The slight reduction in the bulk density is due to the lower specific gravity of the BLA compared to that of OPC [39, 61, 62]. Additionally, the hardened cement pastes with BLA showed lower water absorption and lower porosity especially at 90 days. The better performance of the cement pastes with BLA is due to the combined effect of pozzolanic activity and the filler effect of the BLA, resulting in the refinement of the pores of the cement pastes. Therefore, the reduction of water absorption and total porosity were resulted [40, 42, 60-63]. It is good mention that the rate of the normal hydration process of the OPC is often decreased due to the addition of BLA at the expense of the OPC material. So, the formed amount of CSH was reduced, This was compensated by the pozzolanic reactions among BLA and free lime of $Ca(OH)_2$ resulting from the hydration of calcium silicate phases of the cement.

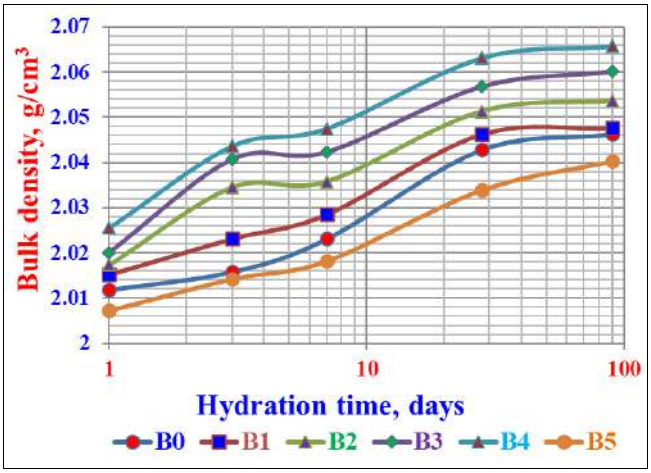

Fig 8: Bulk density of the various cement pastes with and without BLA hydrated up to 90 days.

Chemical properties

Chemically bound water content

The chemically-bound water contents of the various cement pastes with and without BLA (B0-B5) are drawn versus the hydration time in Fig. 9. The bound water content of the blank (B0) was improved and enhanced as the hydration time progressed up to 90 days. This is principally due to the occurrence of the normal hydration process of the major phases of the cement [44, 45]. With the substitution of BLA, the bound water content was further improved and increased till 12% BLA content (B4), and then was suddenly decreased (B6). The decrease of bound water content is distinctly due to the large deficiency of the main binding material of the cement [48-63]. As a result, the optimum BLA content is only 12% (B4). Hence, the higher BLA content is undesirable.

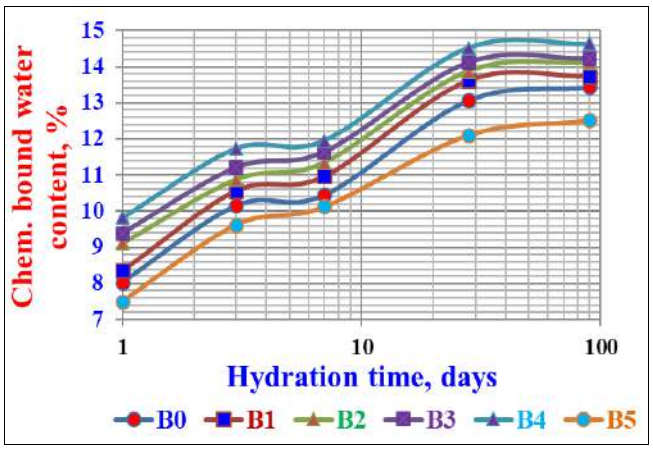

Fig 9: Chemically-bound water content of the various cement pastes with and without BLA hydrated up to 90 days.

Free lime content

The free lime contents of the various cement pastes with and without BLA (B0-B5) hydrated up to 90 days, are drawn as a function of hydration time in Fig. 10. It is clear that the free lime content of the control (B0) gradually increased with the hydration time up to 90 days. This is mainly attributed to the normal hydration of the di- and tricalcium silicates of the cement (C_2S and C_3S) to form CSH [44, 45]. With the incorporation of BLA at the expense of the cement, the free lime content slightly decreased with the time of hydration till 90 days. This is essentially contributed to the pozzolanic reactivity of the BLA with the resulting free lime, $Ca(OH)_2$ forming additional CSH [39, 60, 63].

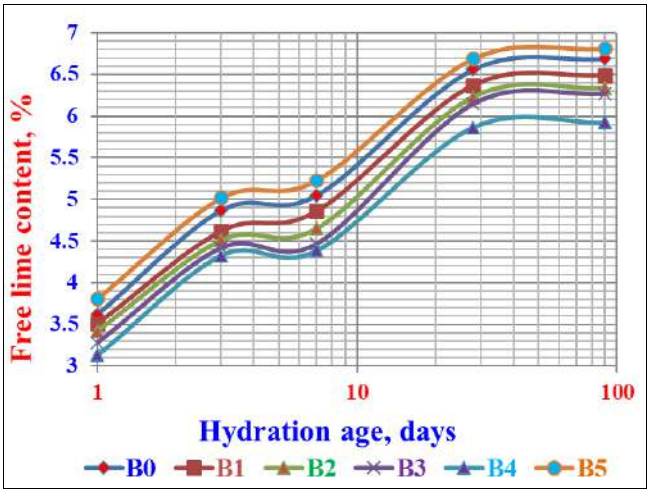

Fig 10: Free lime contents of the various cement pastes with and without BLA hydrated up to 90 days

Mechanical Properties

Compressive strength

The data of compressive strength of the various cement batches containing BLA (B0-B5) hydrated up to 90 days are shown in Fig. 11. Generally, the compressive strengths of the hardened cement pastes increased with hydration time up to 90 days due to the normal hydration process of the main phases of the cement [39, 44, 45, 61]. The compressive strength was further increased as the BLA content increased, but only up to 15% (B4), and then decreased with any further increase of BLA content (B5). Moreover, the increase of the compressive strength is mainly attributed to the filling performance and pozzolanic reactivity of BLA material [48, 59-63], whereas the decrease of compressive strength is due to the detrimental characteristics of the higher specific surface area of BLA that created the agglomeration of the cement particles. This worse performance effect is associated with the lower cement content that influences the direct reduction of the primary hydration products responsible for the compressive strength (CSH) and negatively reflected on the rate of Ca^{2+} release that delaying the precipitation of calcium hydroxide [64]. Therefore, it reduces its availability for the development of pozzolanic reactions with the BLA. Thus, the ideal limit of BLA to be incorporated in the OPC (B0) is 12%, because with the higher percentages (B5), the filler effect of the particles and the availability of $Ca(OH)_2$ in the hydration reaction are reduced [65]. On the other hand, it should be noted that further studies on the kinetics of the reactions at later ages are necessary. The larger specific surface area of BLA causes a microfilling effect resulting in the creation of additional nucleation sites and higher effective proportion of water for cement hydration [57, 66]. Also, the low crystallinity of BLA favors the development of pozzolanic reactions, allowing secondary CSH gel formation to occur. As a result, the combination of these effects, the porous structure of the hardened cement pastes is refined [67]. Consequently, an improvement in compressive strength is observed. It could be concluded that the rate of the normal hydration process of the OPC (B0) is often declined due to the replacement of BLA at the expense of the OPC material. So, the quantity of the formed CSH was reduced, This was compensated by the

pozzolanic reactions between BLA and free lime, Ca $(OH)_2$ coming from the hydration of di- and tricalcium silicate phases of the cement.

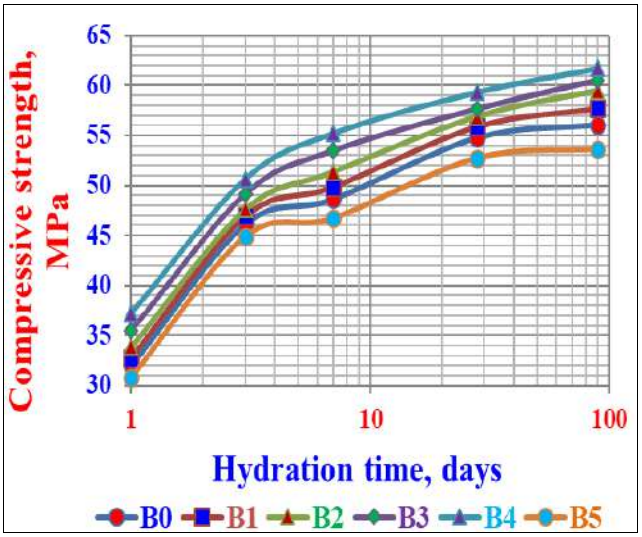

Fig 11: Compressive strength of the various cement pastes with and without BLA hydrated up to 90 days.

FT-IR spectra

The FT-IR spectra of the cement batches B0, B3 and B4 hydrated at 90 days are shown in Fig. 12. The sharp absorption band at wave number 3645-3641 cm^{-1} is related to the free OH^{-1} group coordinated to Ca^{2+}, i.e. free lime, Ca $(OH)_2$, i.e. (CH). The intensity of the free lime absorption band of the control (B0) is detected obviously, which was gradually decreased with the incorporation of BLA (B3 and B4). This is mainly attributed to the active pozzolanic effect of BLA that initiates and improves the rate of hydration [39-41, 60-62, 68]. The broad absorption band intensity at wave number 3789-3015 cm^{-1} which is due to the OH^{-1} group associated to H^+ bond (H_2O) increased with the incorporation of BLA due to the absorption of large quantity of water to form CSH. The intensity of the absorption band of CSH was improved with BLA content. The two absorption bands nearly at 1718-1645 and 1573-1155 cm^{-1} are related to the main silicate band involve Si-O stretching vibration bands of CSH. The three absorption bands at 1120-695 cm^{-1} that are characterizing CO_3^{2-} and SO_4^{2-}, enhanced with BLA content. This may be due to the rate of carbonation and sulfonation of CSH and /or CSAH.

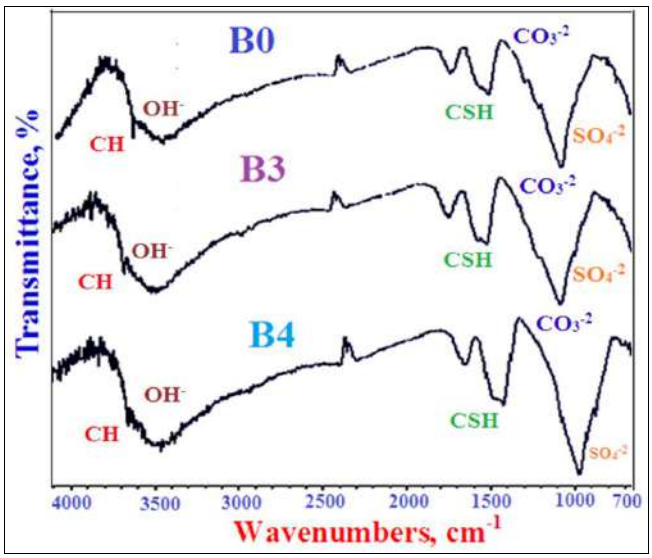

Fig 12: The FT-IR spectra of the cement pastes B0, B3 and B4 hydrated at 90 days.

SEM images

The SEM images of the cement batches B0, B1, B3 and B4 hydrated after 28 days of hydration are shown in Fig. 13. The hydrated phases of cement paste, as trisulphoaluminate hydrate (C_3A. 3 $CaSO_4$. $32H_2O$) or ettringite (AFt) as needle-like crystals, calcium hydroxide (CH) and calcium silicate hydrate (CSH) are clearly observed (P0). The AFt crystals as well as CH content are clearly reduced till completely disappearred with BLA (B4), while CSH increased, i.e. the disappearrance of AFt and CH was compensated by the formation of additional CSH. The SEM image of B4 showed a higher densification due to the lower voids or porosity and the higher formation of CSHs. This is in agreement with the results of physical and chemical properties as bulk density, porosity and compressive strength.

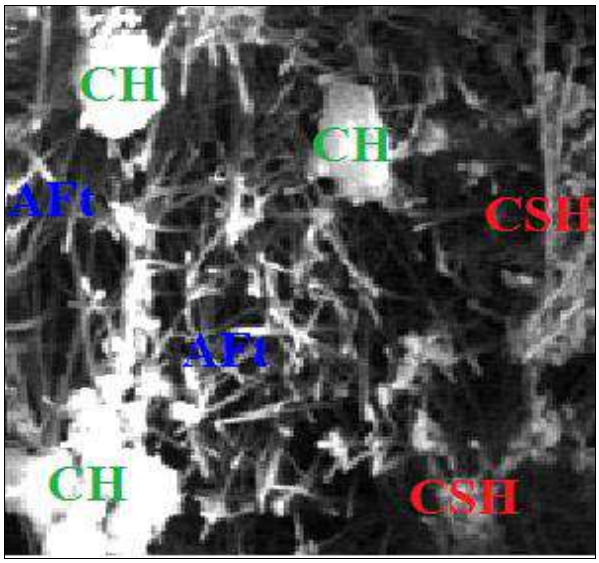

B0

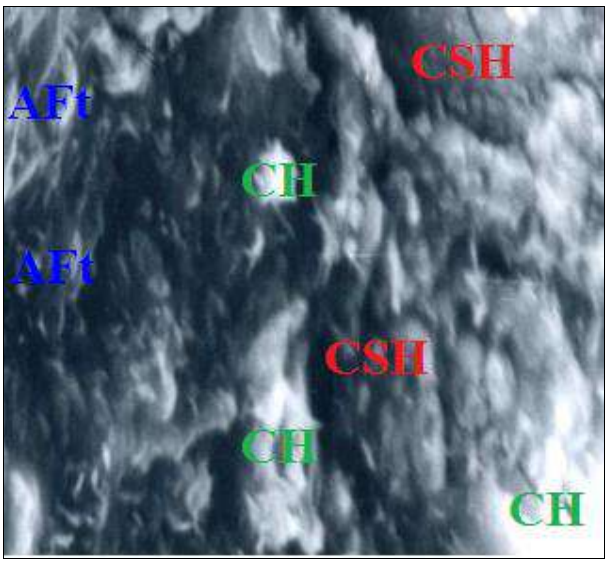

B1

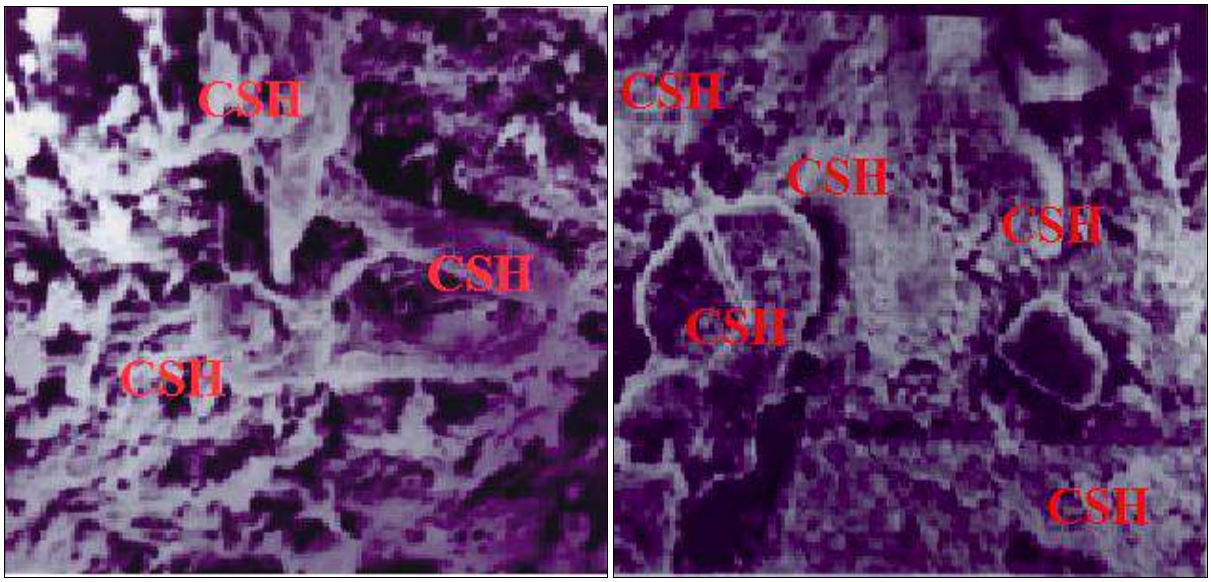

B3 B4

Fig 13: The SEM images of the cement pastes B0, B3 and B4 hydrated at 28 days.

Conclusions

1. Generally, all characteristics of the various cement pastes (B0-B4) are improved with the hydration times up to 90 days due to the normal hydration process.
2. The water of consistency as well as setting times (initial and final) increased with the increase of BLA content.
3. The water absorption and total porosity gradually decreased with the incorporation of BLA till 12%, but then decreased with any further increase.
4. The bulk density improved and enhanced graduallywith the increase of BLA content only up to 12%, and then it was diminished.
5. The bound water content as well as compressive strength improved and enhanced with increase of BLA content up to 12%, and then decreased.
6. The free lime content was decreased with presence of BLA due to the pozzolanic activity of BLA with the free lime released from the hydration of the silicate phases of the cement.
7. So, the optimum content of BLA must not exceed than 12%.
8. 7-The FT-IR spectra as well as SEM images proved that the free lime content decreased with the presence of BLA, while CSH increased.
9. All of the obtained results are in agreement with each other.
10. Also, we are looking to promote the use of agricultural wastes of low values with the ability to contribute to a cleaner production due to the possibility of producing concrete with a smaller carbon footprint. Furthermore, it can guide the development of future research in related fields.

Declaration of Competing Interest

The authors declare that they do not have any commercial or associative interest that represents a conflict of interest in connection with the work submitted.

Acknowledgments

The author gratefully acknowledges the financial support of the National Research Centre.

Fud

This research article is self-sponsored

References

1. Wang Y, Shao Y, Matovic MD, Whalen JK. Recycling combustion ash for sustainable cement production: A critical review with data-mining and time-series predictive models, Constr. Build. Mater. 2016;123:673–689, https://doi.org/10.1016/j.conbuildmat.2016.07.031.
2. Habert G, Miller SA, John VM, Provis JL, Favier A, Horvath A, *et al*. Environmental impacts and decarbonization strategies in the cement and concrete industries, Nature Reviews Earth & Environment. 2020;1(11):559-573. https://doi. org/10.1038/s43017-020-0093-3.
3. Wang D, Shi C, Farzadnia N, Shi Z, Jia H. A review on effects of limestone powder on the properties of concrete, Constr. Build. Mater. 2018;192:153-166, https://doi.org/10.1016/j.conbuildmat.2018.10.119.
4. Scrivener KL, John VM, Gartner EM. Eco-efficient cements: Potential economically viable solutions for a low-CO2 cement-based materials industry, Cem. Concr. Res. 2018;114:2–26, https://doi.org/10.1016/j. cemconres.2018.03.015.
5. Andrew RM. Global CO_2 emissions from cement production, 1928–2018, Earth Syst. Sci. Data. 2019;11(4):1675-1710. https://doi.org/10.5194/essd-11-1675-2019.
6. Zheng C, Zhang H, Cai X, Chen L, Liu M, Lin H, *et al*. Characteristics of CO_2 and atmospheric pollutant emissions from China's cement industry: A life-cycle perspective, J. Cleaner Prod. 2021;282:124533, https://doi.org/10.1016/j. jclepro.2020.124533.
7. Alnahhal MF, Alengaram UJ, Jumaat MZ, Alsubari B, Alqedra MA, Mo KH. Effect of aggressive chemicals on durability and microstructure properties of concrete containing crushed new concrete aggregate and non-traditional supplementary cementitious materials, Constr. Build. Mater. 2018;163:482-495. https://doi.org/10.1016/j.conbuildmat.2017.12.106.

8. Diniz HAA, dos Anjos MAS, Rocha AKA, Ferreira RLS. Effects of the use of agricultural ashes, metakaolin and hydrated-lime on the behavior of self-compacting concretes, Constr. Build. Mater. 2022;319:126087. https://doi.org/10.1016/j.conbuildmat.2021.126087.
9. Fonseca TV, dos Anjos MAS, Ferreira RLS, Branco FG, Pereira L. Evaluation of self-compacting concretes produced with ternary and quaternary blends of different SCM and hydrated-lime, Constr. Build. Mater. 2022;320:126235. https://doi.org/10.1016/j.conbuildmat.2021.126235.
10. Faried AS, Mostafa SA, Tayeh BA, Tawfik TA. The effect of using nano rice husk ash of different burning degrees on ultra-high-performance concrete properties, Constr. Build. Mater. 2021;290:123279, https://doi.org/10.1016/J. CONBUILDMAT.2021.123279.
11. Tayeh BA, Alyousef R, Alabduljabbar H, Alaskar A. Recycling of rice husk waste for a sustainable concrete: A critical review, J. Cleaner Prod. 2021;312:127734, https://doi.org/10.1016/J.JCLEPRO.2021.127734.
12. Faried AS, Mostafa SA, Tayeh BA, Tawfik TA. Mechanical and durability properties of ultra-high performance concrete incorporated with various nano waste materials under different curing conditions, Journal of Building Engineering. 2021;43:102569, https://doi.org/10.1016/J.JOBE.2021.102569.
13. Agwa IS, Omar OM, Tayeh BA, Abdelsalam BA. Effects of using rice straw and cotton stalk ashes on the properties of lightweight self-compacting concrete, Constr. Build. Mater. 2020;235:117541, https://doi.org/10.1016/J. CONBUILDMAT.2019.117541.
14. Anjos MAS, Araújo TR, Ferreira RLS, Farias EC, Martinelli AE. Properties of self-leveling mortars incorporating a high-volume of sugar cane bagasse ash as partial Portland cement replacement, Journal of Building Engineering. 2020;32:101694, https://doi.org/10.1016/j.jobe.2020.101694.
15. de A Mello LC, dos Anjos MAS, de S´a MVVA, de Souza NSL, de Farias EC. Effect of high temperatures on self-compacting concrete with high levels of sugarcane bagasse ash and metakaolin, Construction and Building Materials. 2020;248:118715. https://doi.org/10.1016/j.conbuildmat.2020.118715.
16. Rossignolo JA, Rodrigues MS, Frias M, Santos SF, Junior HS. Improved interfacial transition zone between aggregate-cementitious matrix by addition sugarcane industrial ash, Cem. Concr. Compos. 2017;80:157-167. https://doi. org/10.1016/j.cemconcomp.2017.03.011.
17. Zareei SA, Ameri F, Bahrami N. Microstructure, strength, and durability of eco-friendly concretes containing sugarcane bagasse ash, Constr. Build. Mater. 2018;184:258-268, https://doi.org/10.1016/j.conbuildmat.2018.06.153.
18. Hafez RDA, Tayeh BA, Abdelsamie K. Manufacturing nano novel composites using sugarcane and eggshell as an alternative for producing nano green mortar, Environmental Science and Pollution, Research. 2022;29:34984-35000. https:// doi.org/10.1007/S11356-022-18675-4/FIGURES/17.
19. Amin M, Zeyad AM, Tayeh BA, Saad Agwa I. Effects of nano cotton stalk and palm leaf ashes on ultrahigh-performance concrete properties incorporating recycled concrete aggregates, Constr. Build. Mater. 2021;302:124196. https:// doi.org/10.1016/J.CONBUILDMAT.2021.124196.
20. Karim MR, Hashim H, Abdul Razak H. Assessment of pozzolanic activity of palm oil clinker powder, Constr. Build. Mater. 2016;127:335–343. https://doi.org/ 10.1016/j.conbuildmat.2016.10.002.
21. Khankhaje E, Hussin MW, Mirza J, Rafieizonooz M, Salim MR, Siong HC, *et al*. On blended cement and geopolymer concretes containing palm oil fuel ash, Mater. Des. 2016;89:385-398. https://doi.org/10.1016/j. matdes.2015.09.140.
22. Hamada H, Tayeh B, Yahaya F, Muthusamy K, Al-Attar A. Effects of nano-palm oil fuel ash and nano-eggshell powder on concrete, Constr. Build. Mater. 2020;261:119790, https://doi.org/10.1016/J.CONBUILDMAT.2020.119790.
23. Hamada HM, Skariah Thomas B, Tayeh B, Yahaya FM, Muthusamy K, Yang J. Use of oil palm shell as an aggregate in cement concrete: A review, Construction and Building Materials. 2020;265:120357. https://doi.org/10.1016/J. CONBUILDMAT.2020.120357.
24. Hamada HM, Al-attar AA, Yahaya FM, Muthusamy K, Tayeh BA, Humada AM. Effect of high-volume ultrafine palm oil fuel ash on the engineering and transport properties of concrete, Case Stud. Constr. Mater. 2020;12:e00318. https://doi.org/10.1016/j.cscm.2019.e00318
25. Zeyad AM, Johari MAM, Alharbi YR, Abadel AA, Amran YHM, Tayeh BA, *et al*. Influence of steam curing regimes on the properties of ultrafine POFA-based high-strength green concrete, Journal of Building Engineering. 2021;38:102204, https://doi.org/10.1016/J.JOBE.2021.102204.
26. Zeyad AM, Azmi Megat Johari M, Abutaleb A, Tayeh BA. The effect of steam curing regimes on the chloride resistance and pore size of high–strength green concrete, Construction and Building Materials. 2021;280:122409. https://doi. org/10.1016/J.CONBUILDMAT.2021.122409.
27. Hamada HM, Alattar AA, Yahaya FM, Muthusamy K, Tayeh BA, Hamada HM, *et al*. Mechanical properties of semi-lightweight concrete containing nano-palm oil clinker powder, Physics and Chemistry of the Earth, Parts A/B/C. 2021;121:102977, https://doi. org/10.1016/J.PCE.2021.102977.
28. Chowdhury S, Maniar A, Suganya OM. Strength development in concrete with wood ash blended cement and use of soft computing models to predict strength parameters, J. Adv. Res. 2015;6:907-913. https://doi.org/10.1016/j. jare.2014.08.006.
29. Siddique R. Utilization of Industrial By-products in Concrete, Procedia Eng. 2014;95:335–347, https://doi.org/10.1016/j.proeng.2014.12.192.
30. Velay-Lizancos M, Azenha M, Martínez-Lage I, V´azquez-Burgo P. Addition of biomass ash in concrete: Effects on E-Modulus, electrical conductivity at early ages and their correlation, Constr. Build. Mater. 2017;157:1126–1132, https://doi. org/10.1016/j.conbuildmat.2017.09.179.
31. Cordeiro GC, Sales CP. Pozzolanic activity of elephant

grass ash and its influence on the mechanical properties of concrete, Cem. Concr. Compos. 2015;55:331-336. https://doi.org/10.1016/j.cemconcomp.2014.09.019.
32. Hilal N, Mohammed Ali TK, Tayeh BA. Properties of environmental concrete that contains crushed walnut shell as partial replacement for aggregates, Arabian J. Geosci. 2020;13(16):1-9. https://doi.org/10.1007/S12517-020-05733-9.
33. Tayeh BA, Hadzima-Nyarko M, Zeyad AM, Al-Harazin SZ. Properties and durability of concrete with olive waste ash as a partial cement replacement, Advances in Concrete, Construction. 2021;11(1):59-71. https://doi.org/10.12989/ ACC.2021.11.1.059.
34. Zhou S, Tang W, Xu P, Chen X. Effect of cattle manure ash on strength, workability and water permeability of concrete, Constr. Build. Mater. 2015;84:121-127. https://doi.org/10.1016/j.conbuildmat.2015.03.062.
35. Kanning RC, Portella KF, Da Costa MRM, Puppi RFK. in: Evaluation of Pozzolanic Activity of Banana Leaf Ash, in, in-house publishing, XII-DBMC Intern. Conf. Durability of Build. Mat. and Comp. Porto, Portugal, 2011, 1-8.
36. Kanning RC, Portella KF, Bragança MOGP, Bonato MM, Dos Santos JCM. Banana leaves ashes as pozzolan for concrete and mortar of Portland cement, Constr. Build. Mater. 2014;54:460-465. https://doi.org/10.1016/j. conbuildmat.2013.12.030.
37. Luhar S, Luhar I, Abdullah MMAB, Hussin K. Challenges and prospective trends of various industrial and solid wastes incorporated with sustainable green concrete, Advances in Organic Farming, 2021, 223-240, https://doi.org/ 10.1016/B978-0-12-822358-1.00001-8.
38. Voora V, Larrea C, Bermudez S. Global Market Report: Bananas; c2020. https:// www.iisd.org/publications/global-market-report-bananas. 2.
39. Darweesh HHM. Influence of sun flower stalk ash (SFSA) on the behavior of Portland cement pastes, Results in Engineering. 2020;8:100171. https://doi.org/10.1016/j.rineng.2020.100171.
40. Darweesh HHM. Utilization of Physalis Pith Ash as a Pozzolanic Material in Portland Cement Pastes, Journal of Biomaterials. 2020;5(1):1-9. http://www.sciencepublishinggroup.com/j/jb
41. Darweesh HHM. Characterization of Coir Pith Ash Blended Cement Pastes, Research & Development in Material science, RDMS.000851. 2021;15(1). DOI: 10.31031/RDMS.2021.15.000851.
42. Darweesh HHM. Water Permeability, Strength Development And Microstructure of Activated Pulverized Rice Husk Ash Geopolymer Cement, Nano NEXT. 2022;3(1):5-22. https://doi.org/10.54392/nnxt2212.
43. ASTM-Standards C170-90. Standard Test Method for Compressive Strength of Dimension Stone, 1993, 828-830.
44. Neville AM. Properties of Concrete, 5th Edn, Longman Essex, UK; c2011.
45. Hewlett PC, Liska M. Lea's Chemistry of Cement and Concrete, Butterworth- Heinemann, London; c2017.
46. Darweesh HHM. Mortar Composites Based on Industrial Wastes, International Journal of Materials Lifetime, 2017;3(1):1-8. http://pubs.sciepub.com/ijml/3/1/1.
47. Lux´an MP, Madruga F, Saavedra J. Rapid evaluation of pozzolanic activity of natural products by conductivity measurement, Cem. Concr. Res. 1989;19(1):63–68, https://doi.org/10.1016/0008-8846(89)90066-5.
48. Pay´a J, Borrachero M, Monz ´o J, Peris-Mora E, Amahjour F. Enhanced conductivity measurement techniques for evaluation of fly ash pozzolanic activity, Cem. Concr. Res. 2001;31:41-49. https://doi.org/10.1016/S0008-8846(00) 00434-8.
49. Snellings R, Li X, Avet F, Scrivener K, Rapid A. Robust, and Relevant (R3) Reactivity Test for Supplementary Cementitious Materials, ACI Materials Journal. 116 (2019). https://doi.org/10.14359/51716719.
50. McCarthy MJ, Dyer TD. Pozzolanas and Pozzolanic Materials, in: Lea's Chemistry of Cement and Concrete, Elsevier, 2019, 363-467. https://doi.org/ 10.1016/B978-0-08-100773-0.00009-5.
51. Martirena F, Monz´o J. Vegetable ashes as Supplementary Cementitious Materials, Cem. Concr. Res. 2018;114:57–64, https://doi.org/10.1016/j. cemconres.2017.08.015.
52. ASTM C618-12, Standard Specification for Coal Fly Ash and Raw or Calcined Natural Pozzolan for Use. 2000;4:1-4. https://doi.org/10.1520/C0618.
53. Sims I, Lay J, Ferrari J. Concrete Aggregates, in: Lea's Chemistry of Cement and Concrete, Elsevier, 2019, 699-778. https://doi.org/10.1016/B978-0-08- 100773-0.00015-0.
54. Marvila MT, de Azevedo ARG, de Matos PR, Monteiro SN, Vieira CMF. Rheological and the Fresh State Properties of Alkali-Activated Mortars by Blast Furnace Slag, Materials. 2021;14:2069, https://doi.org/10.3390/ma14082069.
55. Aitcin PC. Supplementary cementitious materials and blended cements, in: Science and Technology of Concrete Admixtures, Elsevier, 2016, 53-73. https://doi.org/10.1016/B978-0-08-100693-1.00004-7.
56. Pagliari L, Dapiaggi M, Pavese A, Francescon F. A kinetic study of the quartz–cristobalite phase transition, J. Eur. Ceram. Soc. 2013;33(15-16):3403–3410, https://doi.org/10.1016/j.jeurceramsoc.2013.06.014.
57. Singh RK, Pandey D, Patil T, Sawarkar AN. Pyrolysis of banana leaves biomass: Physico-chemical characterization, thermal decomposition behavior, kinetic and thermodynamic analyses, Bioresour. Technol. 2020;310:123464, https://doi. org/10.1016/j.biortech.2020.123464.
58. Kumar M, Shukla SK, Upadhyay SN, Mishra PK. Analysis of thermal degradation of banana (Musa balbisiana) trunk biomass waste using iso-conversional models, Bioresour. Technol. 2020;310:123393, https://doi.org/ 10.1016/j.biortech.2020.123393.
59. de Azevedo Basto P, Junior HS, de Melo Neto AA. Characterization and pozzolanic properties of sewage sludge ashes (SSA) by electrical conductivity. Cement and Concrete Composites. 2019 Nov 1;104:103410. https://doi.org/10.1016/j. cemconcomp.2019.103410.
60. HHM Darweesh. Geopolymer Cement Based on Bioactive Egg Shell Waste or Commercial Calcium Carbonates, Research & Development in Material science, RDMS.000901. 2022;17(1):1907-1916.

https://doi.org/10.31031/RDMS.2022.17.000901
61. Darweesh HHM. Physico-mechanical properties and microstructure of Portland cement pastes replaced by corn stalk ash (CSA), International Journal of Chemical Research and Development. 2022;2(1):24-33. www.chemicaljournal.in
62. Darweesh HHM, Abo El Suoud MR. Effect of Agricultural Waste Material on the Properties of Portland Cement Pastes, Research & Development in Material science, RDMS.000802. 2020;13(1):1360-1367. https://doi.org/10.31031/RDMS.2020.13.000802
63. Le HT, Ludwig HM. Effect of rice husk ash and other mineral admixtures on properties of self-compacting high performance concrete, Mater. Des. 2016;89:156-166, https://doi.org/10.1016/j.matdes.2015.09.120.
64. de Matos PR, Sakata RD, Onghero L, Uliano VG, de Brito J, Campos CEM, Gleize PJP. Utilization of ceramic tile demolition waste as supplementary cementitious material: An early-age investigation, Journal of Building Engineering. 2021;38:102187. https://doi.org/10.1016/j.jobe.2021.102187.
65. Somna R, Jaturapitakkul C, Rattanachu P, Chalee W. Effect of ground bagasse ash on mechanical and durability properties of recycled aggregate concrete, Materials & Design (1980-2015). 2012;36:597-603. https://doi.org/10.1016/j. matdes.2011.11.065.
66. Lothenbach B, Scrivener K, Hooton RD. Supplementary cementitious materials, Cem. Concr. Res. 2011;41(12):1244–1256. https://doi.org/10.1016/j.cemconres.2010.12.001.
67. Le HT, Ludwig HM. Effect of rice husk ash and other mineral admixtures on properties of self-compacting high performance concrete, Mater. Des. 2016;89:156-166. https://doi.org/10.1016/j.matdes.2015.09.120.
68. Darweesh HHM, Abo El-Suoud MR. Palm Ash as a Pozzolanic Material for Portland Cement Pastes, To Chemistry Journa. 2019;4:72-85. ISSN: 2581-7507. http://purkh.com/index.php/tochem